

## Ion Channel Properties and Episodic Activity in Isolated Immortalized Gonadotropin-Releasing Hormone (GnRH) Neurons

Martha M. Bosma

Department of Physiology and Biophysics, University of Washington School of Medicine, SJ-40, Seattle, Washington 98195

Received: 16 March 1993

**Abstract.** The mechanism of periodic gonadotropin-releasing hormone (GnRH) secretion from hypothalamic neurons is difficult to elucidate due to the diffuse distribution of GnRH neurons and the complex interaction of neuronal inputs onto them. Recent use of transgenic techniques allowed construction of an immortalized GnRH neuronal cell line (GT1), which has neuronal markers and secretes GnRH in a periodic fashion. Using the patch-clamp recording technique in the whole-cell and nystatin perforated-patch configuration, the present experiments show that this cell line expressed a tetrodotoxin-sensitive Na channel, two types of Ca channels, three types of outward K channels and a K inward rectifier. The latter current was suppressed in some cells by GnRH or somatostatin. In addition, a gamma-aminobutyric acid (GABA) response, presumably through GABA<sub>A</sub> receptors, is recorded. In long-term current-clamp recordings, spontaneous depolarizing activity was found to increase, and then decrease, between 20–35 min after removal of the cells from serum- and steroid-containing medium. In some cases, more than one cycle of activity was seen. Under voltage clamp, an inward current was recorded at similar times, with reversal at about –15 mV. Thus, two mechanisms of cell interaction, GABA<sub>A</sub> responses and feedback through GnRH responses, and one mechanism of endogenous periodic electrical activity were observed in these cells, which could synchronize periodic GnRH release.

**Key words:** Hypothalamus — Neuron — Inward rectifier — Periodic activity — GnRH neuron

### Introduction

Gonadotropin-releasing hormone (GnRH) is a major point of control in the hypothalamic-pituitary-gonadal axis. GnRH is released in a periodic fashion in all mammals studied [3, 17, 25], eliciting periodic secretion of luteinizing hormone (LH) from pituitary gonadotropes [5, 7, 25]. This LH secretion is strongly correlated in timing with electrical activity recorded from mediobasal hypothalamic neurons [31]. Although there is much evidence that neuronal feedback [14, 28], gonadal feedback [24] and auto feedback of GnRH itself [27, 34] all modulate the secretion of GnRH, it is not clear what the origin of the periodic activity is. Experiments with isolated mediobasal hypothalamic pieces have shown that many of the neuronal inputs are not needed for periodic secretion [23, 25]. However, homogeneous cultures of primary GnRH neurons have not been established because of the diffuse localization of the neurons within the CNS [26, 32]. Thus, the mechanism of the origin of the periodic secretion is not known.

Recently, an immortalized cell line has been made [22] by linking the GnRH promoter gene to the SV40 T-antigen gene, and injecting the fused gene into fertilized mouse eggs to generate transgenic mice. Several mice developed CNS tumors, and one such tumor was used to derive three clonal neurosecretory cell lines (GT1-1, GT1-3, GT1-7). These cell lines carry neuronal (and not glial) markers [22], synthesize GnRH and GnRH-associated protein (GAP) [19, 29], secrete GnRH in a periodic fashion [20, 30], and are able to modify GnRH secretion in response to activin-A and endothelin [8, 15]. Because GnRH secretion from these clonal cell lines is periodic, the oscillator that gener-

Correspondence to: Department of Pharmacology, University of Washington School of Medicine, SJ-30, and GRECC, VAMC, Seattle, Washington 98195

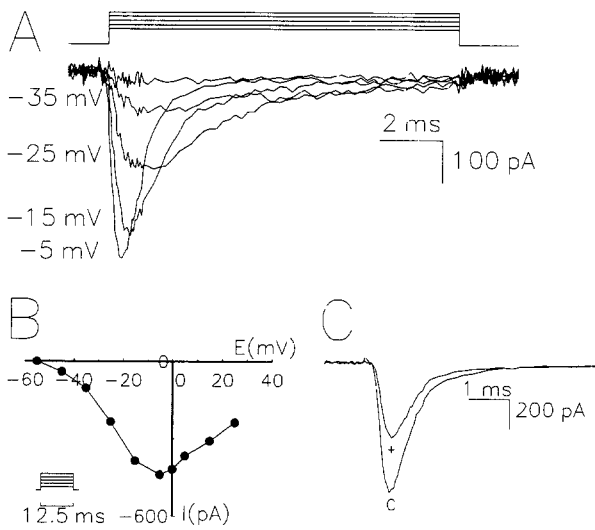


**Fig. 1.**  $\text{Na}^+$  currents in GT1-7 cells. (A) Inward  $\text{Na}^+$  currents elicited by 12.5 msec steps from  $-115$  mV to potentials indicated. Lines above indicate pulse protocol. (B) Current-voltage relation for currents from cell in part A. Peak current during the pulse was measured and plotted against voltage. (C) Currents elicited by steps to  $+5$  mV without (c) and with (+)  $2.5$  nM TTX.

ates the periodic behavior can be localized to the intrinsic network of the GnRH cells themselves [20, 30]. I have used these GnRH cells to investigate the properties and modulation of ionic conductances which may be involved in GnRH secretion and to explore the possibility of an underlying endogenous electrical rhythm related to periodic secretion.

## Materials and Methods

### CELL CULTURE

GT1-3 and GT1-7 cells were kindly given to us by Dr. Pamela Mellon (Salk Institute). The cells were cultured in DME medium supplemented with 5% horse serum and 5% fetal calf serum, to which was added 1% penicillin-streptomycin. Stock 100-mm tissue culture dishes were subcultured every 5–7 days when cells reached 70% confluency. Cells were grown at low density (10% confluency) on 35 mm culture dishes for electrophysiology experiments. Cell-culture reagents were obtained from GIBCO. The majority of voltage-clamp characterization of currents was done in GT1-3 cells, and was confirmed in GT1-7 cells. The GT1-7 cells were more robust and easier to patch clamp, and were used for all long-term nystatin perforated-patch recordings.

### ELECTROPHYSIOLOGICAL RECORDING

Electrophysiological experiments were performed 2 days after the cells were plated into 35-mm dishes. Tissue culture medium was removed and the cells bathed in zero-divalent solution for 30 sec before flowing in normal Ringer. The zero-divalent wash

increased the success of obtaining Gohm seals on the cells. A chamber was constructed inside the tissue culture dish to reduce total bath volume by sealing a Sylgard (Dow, Midland, MI) ring to the bottom of the dish. Total bath volume was 150–200  $\mu\text{l}$ . Bath solutions were changed by perfusing 15–25 vol of the new solution through the chamber or by switching to a different input line on a continuous flow system. The results obtained were similar in the two conditions. Dishes were placed on the stage of a Nikon Diaphot inverted microscope and viewed under Hoffman Modulation Contrast optics. Many cells had obvious neurites extending from them. In denser cultures, networks of neurites were seen. To avoid electrical artifacts caused by cell-to-cell coupling, and to maintain spatial voltage control, whole-cell electrophysiological measurements were made only on cells that did not touch each other and that had no long processes. In about 50% of attempts, if seals could be formed, the patch could be broken to obtain whole-cell recording. The usual duration of recordings was 10–15 min, although some lasted as long as 30–35 min. Recordings with the nystatin perforated-patch technique [11] lasted up to two hours. The measured membrane capacitance of the cells (an electrical measure of their membrane surface area) was  $6.5 \pm 2.3$  pF (mean  $\pm$  SD; equivalent to 650  $\mu\text{m}^2$  of membrane), with a range of 2 to 15 pF ( $n = 188$ ). Capacitance was determined at the beginning and the end of the experiment and did not change. Currents were recorded using a List EPC-7 patch-clamp amplifier (Medical Systems, Greenvale, NY). Voltage pulses were generated and resultant currents recorded in real time, using the BASIC-FASTLAB system of software and hardware (Indec Systems, Capitola, CA). For long-term nystatin recording, the data were digitally sampled onto a VCR and also recorded on a chart recorder. In experiments with sodium currents, leak and capacity currents were subtracted automatically using a P/4 pulse protocol [2]. All reported membrane potentials were corrected for junction potentials of  $-3$  to  $-18$  mV between the pipette solutions and the bath. To indicate the range of single-cell properties encountered, measurements are given as mean  $\pm$  SD, except as indicated.

### SOLUTIONS

For measuring  $\text{Na}^+$  currents, the solutions were (in mM): External: 150 NaCl, 2.5 KCl, 4  $\text{MgCl}_2$ , 10 HEPES, 8 glucose. Internal: 120 CsCl, 3  $\text{MgCl}_2$ , 10 EGTA, 25 HEPES, 2.5 ATP, 0.2 GTP, 0.1 leupeptin. For recording  $\text{K}^+$  currents, the solutions were: External: 2.5 KCl, 150 N-methyl-D-glucamine (NMDG), 1  $\text{MgCl}_2$ , 3  $\text{CaCl}_2$ , 10 HEPES, 8 glucose. Internal: 100 K-aspartate, 20 KCl, 25 HEPES, 10 EGTA, 3  $\text{MgCl}_2$ , 2.5 ATP, 0.2 GTP, 0.1 leupeptin. For  $\text{K}^+$ -selectivity experiments,  $\text{K}^+$  was increased with a concomitant decrease in NMDG. For recording  $\text{Ba}^{2+}$  currents in Ca channels, the solutions were: External: 30  $\text{BaCl}_2$ , 109 NMDG, 2.5 KCl, 1  $\text{MgCl}_2$ , 10 HEPES, 8 glucose. Internal: as for sodium currents. Normal mammalian Ringer consisted of: 150 NaCl, 2.5 KCl, 1  $\text{MgCl}_2$ , 3  $\text{CaCl}_2$ , 10 HEPES and 8 glucose. Zero-divalent solution consisted of: 156 NaCl, 2.5 KCl, 10 HEPES and 8 glucose. All solutions were titrated to pH 7.4 using NaOH or HCl for external solutions and CsOH or KOH for internal solutions, as appropriate.

Nystatin perforated-patch solutions were as follows: fresh stock solutions of nystatin at 50 mg/ml in dimethylsulfoxide were made and used for only 3–4 hr. A solution of 25 mg/ml Pluronic F-127 (a dispersing agent; Molecular Probes, Eugene, OR) in DMSO was dissolved at  $40^\circ\text{C}$  for 10 min, and kept at  $-20^\circ\text{C}$  for 2–3 weeks. Pipette solutions were made by diluting first pluronic,

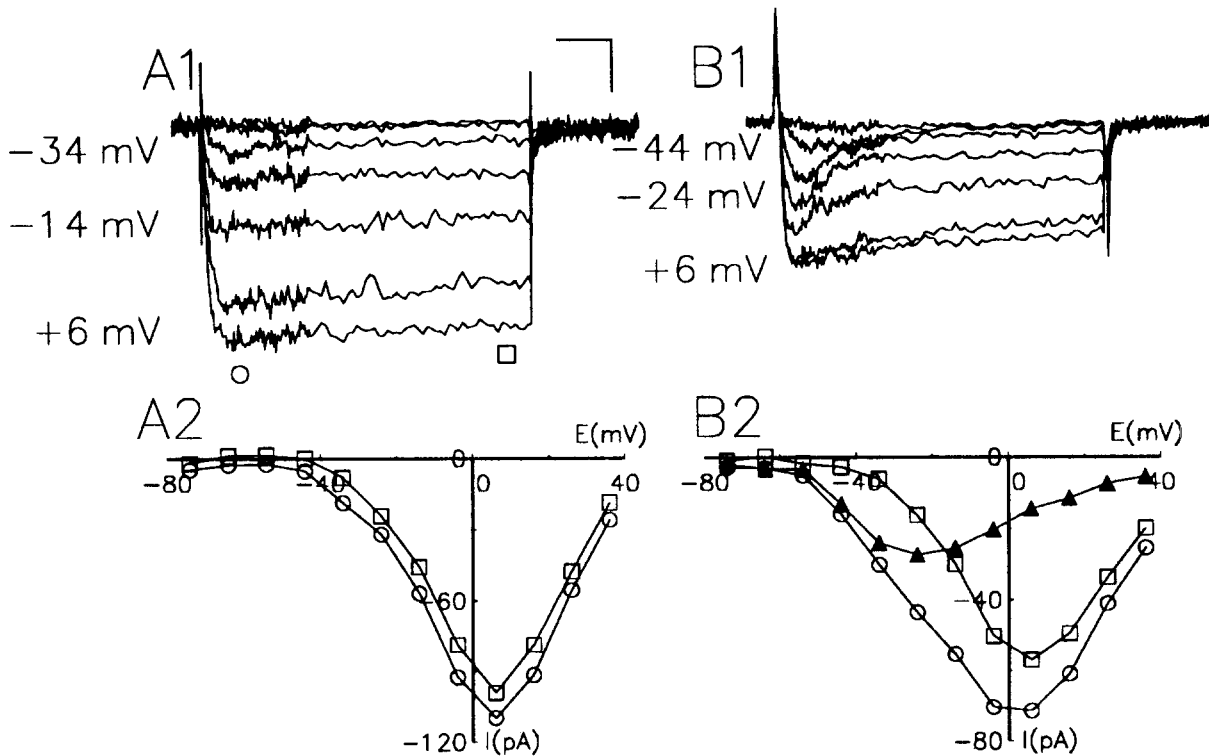


**Fig. 2.** Two types of  $\text{Ba}^{2+}$  currents in GT1-7 cells. (A1) Currents elicited by steps from holding potential of  $-94$  mV to potentials indicated. (A2) Current-voltage relation for peak (circles) and sustained (squares) current measured from above traces. (B1) Currents recorded from a different cell, to similar potential steps. (B2) Current-voltage relation as in A2, with isolated transient current (filled triangles) obtained by subtraction of sustained current from total peak current (circles-squares). Scale bars are 20 msec, 25 pA.

then the nystatin to final concentrations of 0.5 mg/ml each. In some cases, the internal solutions were sonicated before each pipette was filled, but this did not consistently improve the success of the technique. The entire pipette was filled with the nystatin internal solution by backfilling. Patch perforation usually took from 3–10 min, during which pulses were recorded to monitor the progress of perforation by noting the change in access to the membrane capacitance of the cell. Typical series resistances in nystatin perforation were 10–30  $\text{M}\Omega$ .

Peptides used were obtained from Peninsula and 100 mM stock solution was stored at  $-20^\circ\text{C}$ ; other hormones, tetrodotoxin, tetraethylammonium (TEA), 4-aminopyridine (4-AP) and most reagent salts were from Sigma. The dihydropyridine blocker PN200-110 was kindly given to us by Dr. W. Catterall, Dept. of Pharmacology, University of Washington, Seattle. All experiments were done at  $22$ – $24^\circ\text{C}$ .

## Results

### SODIUM CHANNELS

The presence of sodium channels was determined by using a  $\text{Cs}^+$  solution in the pipette and a  $\text{Ca}^{2+}$ -free external solution. Inward  $\text{Na}^+$  currents were seen when the voltage was stepped from a holding

potential of  $-115$  mV to potentials between  $-45$  and  $+25$  mV (Fig. 1A). The currents were rapidly activating and inactivating near the peak potential of  $-15$  to  $-5$  mV. Figure 1B shows the current-voltage relation for this cell; peak current is plotted against the voltage applied during the step from  $-115$  mV. Recorded current from 35 cells averaged  $-560 \pm 378$  pA, or when calculated as current density,  $-112 \pm 93$  pA/pF. The sodium current was blocked by tetrodotoxin (TTX; Fig. 1C) with a  $K_i$  of 2.3 nM (fit of 14 cells, Hill coefficient 0.76). Prepulses (100 msec) to depolarizing potentials inactivated the sodium current; this steady-state inactivation (*data not shown*) was fitted by a Boltzmann equation with a midpoint at  $-47 \text{ mV} \pm 7 \text{ mV}$ , and a slope factor corresponding to an  $e$ -fold change in inactivation every  $8.6 \pm 0.8$  mV ( $n = 5$ ).

### CALCIUM CHANNELS

Because these cells are neurosecretory, it is important to consider the types of calcium channels present and the role that they may play in hormone secretion and modulation of excitability. An external

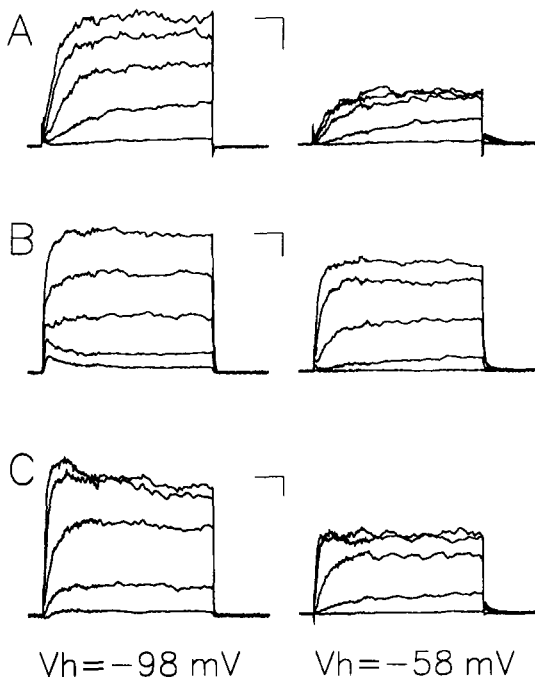


**Fig. 3.** Examples of three types of  $K^+$  current. All portions of the figure show currents during steps to  $-28$ ,  $-8$ ,  $+12$ ,  $+32$ ,  $+52$  mV. (A) Cell with only slowly activating, sustained type of delayed rectifier. Current is smaller from holding potential of  $-58$  mV. (B) Example of cell expressing early transient current (e.g., at  $-28$  and  $-8$  mV) together with the delayed rectifier. This current is not activatable from holding potential of  $-58$  mV. (C) Cell with delayed rectifier and later slower transient current (e.g., at  $+32$  and  $+52$  mV). Both currents are reduced by holding at  $-58$  mV. Scale bars are 30 msec, 100 pA.

solution containing 0 mM  $Na^+$  and 30 mM  $Ba^{2+}$  (which permeates well through Ca channels) and a  $Cs^+$ -containing internal solution were used. Figure 2A1 shows currents elicited from a holding potential of  $-94$  mV to steps ranging from  $-24$  to  $+6$  mV. The current activates within 20 msec and inactivates little during the 120-msec pulse. Figure 2A2 shows the current-voltage relation for these currents; the circles are the peak current within the first 50 msec, and the squares are the average of the last 30 msec of the test potential step. The two curves are similar and peak at the same voltage suggesting that a homogeneous group of high-voltage activated (HVA) Ca channels [1] dominates the calcium current in this cell. However, in Fig. 2B1, currents recorded from a different cell demonstrate that there was sometimes an inactivating component of inward current at the more negative potentials (e.g.,  $-44$  mV). This is seen in the current-voltage relation in Fig. 2B2 as a slight increase in peak current (circles) at more negative potentials, and is seen more clearly by subtracting the sustained current (end of the pulse) from

the peak, resulting in the curve shown by filled triangles. This transient component of current is most likely contributed by a separate channel. On average, the contribution of transient current is quite small. From a holding potential of  $-94$  mV, the sustained current at a test potential of  $+6$  mV was  $-56 \pm 50$  pA/cell ( $n = 52$ ; density  $-10 \pm 8$  pA/pF,  $n = 50$ ). At a test potential of  $-24$  mV, the transient current is activated in relative isolation from the sustained current. The mean transient current at that potential was  $-4.3 \pm 3.5$  pA (range  $-25$  to  $0$  pA; density  $-0.8 \pm 0.9$  pA/pF). In addition, 13/52 cells had  $<1$  pA of inward current at  $-24$  mV. Thus, most of the  $Ba^{2+}$  current is contributed by the sustained Ca channels.

When the holding potential was changed to  $-54$  mV, the sustained component was  $-41 \pm 29$  pA/cell (density  $-8 \pm 5$  pA/pF,  $n = 21$ ), while the transient current was not present at all. Thus, the transient current had a strong dependence on holding potential, whereas the sustained current had a weak dependence. The steady-state inactivation curve for the transient current was fitted by a Boltzmann equation with a half-maximal voltage of  $-67.3$  and a slope factor of an  $e$ -fold change in  $7.4$  mV ( $n = 2$ ; current measured at  $-24$  mV where the sustained current is minimally activated).

The sustained  $Ba^{2+}$  current was reduced to 50% by 20 nM of the dihydropyridine antagonist PN200-110 ( $n = 3$ ), and completely blocked by 100 nM. Thus, these sustained channels are dihydropyridine sensitive. This current was also completely blocked by 100  $\mu$ M  $Cd^{2+}$  ( $n = 2$ ), while some of the transient current remained at 100  $\mu$ M and was more fully blocked at 500  $\mu$ M  $Cd^{2+}$ . The sustained current was labile; the time course of the rundown or washout of current was fitted to a single exponential curve, with a mean  $\tau$  of 423 sec ( $n = 4$ ). The transient component was stable and did not wash out during the course of the recording.

Several hormones implicated in modulation of the GnRH-pituitary system were tested for possible effects on  $Ba^{2+}$  currents. Adenosine (1–20  $\mu$ M) suppressed the current in 8/14 cells tested; gamma-aminobutyric acid (GABA) (2–20  $\mu$ M) suppressed the current in 2/8 cells tested; GnRH (10 nM–1  $\mu$ M) augmented the current in 2/8 cells tested. However, these hormone effects were too inconsistent to study further. In addition, modulation by dibutyl cAMP, a membrane-permeant analogue of cAMP was tested, with negative results (1 mM; 3 cells).

#### OUTWARD POTASSIUM CHANNELS

At least three components of outward current, one sustained and two transient, were recorded from GT1 cells. These were expressed differentially

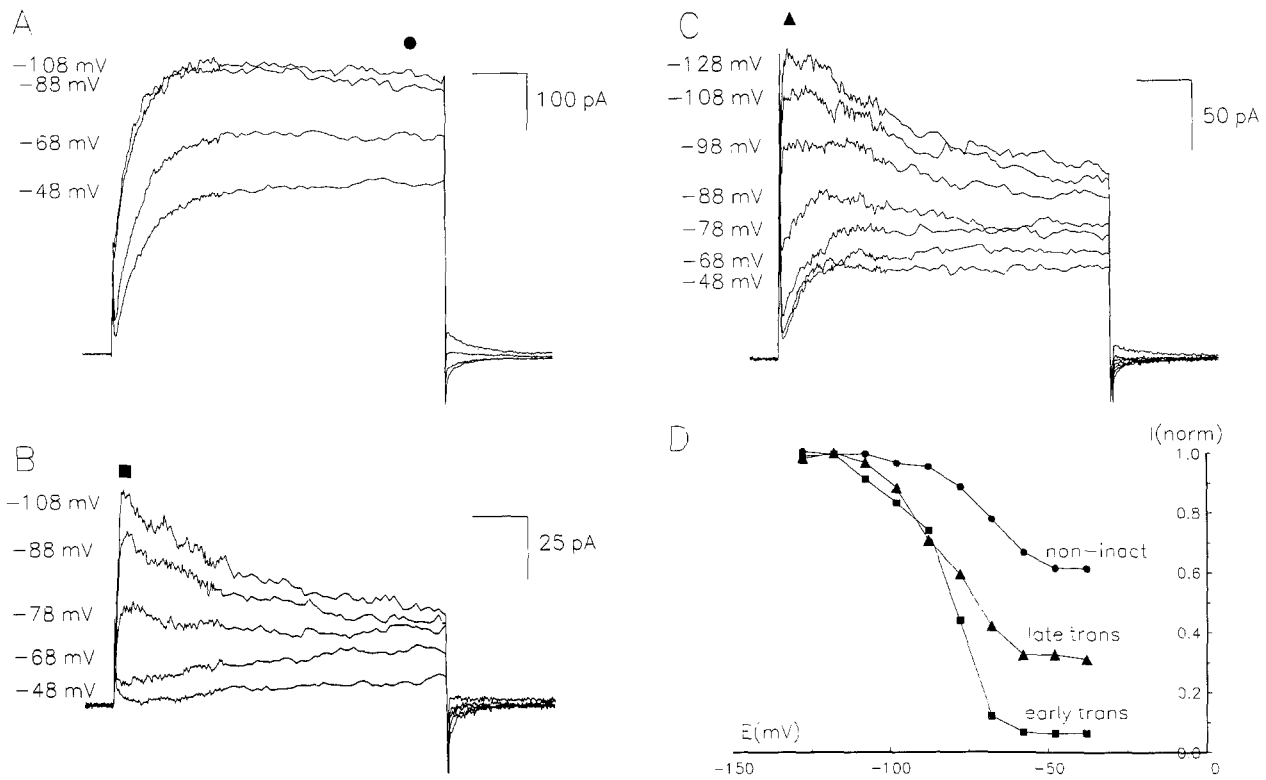


**Fig. 4.** Voltage dependence of steady-state inactivation for the three types of  $K^+$  current. (A) Steps to  $+32$  mV from various holding potentials indicated next to traces in a cell expressing only sustained current. (B) Steps to  $-18$  mV where the sustained current is minimally activated to show effects of holding potential on early transient current. (C) Steps to  $+32$  mV for a cell expressing the steady current and the late transient current. (D) Plots of data from sustained (A; circles) or peak (B, C; squares, triangles) portion of currents. Normalized current plotted against voltage. Horizontal scale bars in A, B and C are 30 msec.

among cells and could be separated on the basis of voltage dependence and pharmacology. With recording conditions that included a pipette solution with K-aspartate and an external solution in which the  $Na^+$  was replaced by NMDG, all cells expressed a slowly activating, sustained delayed-rectifier  $K^+$  current (Fig. 3A). The time constants ( $\tau$ ) of activation of this current ranged from 56 msec at  $-8$  mV to 19 msec at  $+52$  mV. The current measured at the end of a 180 msec pulse to  $+52$  mV was  $394 \pm 189$  pA ( $V_H = -98$  mV;  $n = 70$ ; current density  $61 \pm 23$  pA/pF). This conductance began to activate near  $-23$  mV and reached a maximum at  $+22$  mV, with a midpoint of the activation curve at  $-7.3$  mV and a slope factor of  $e$ -fold in 9.4 mV when fitted with a Boltzmann function. The current had some dependence on holding potential (*see below*) but was still 50% available from a holding potential of  $-58$  mV; 14/65 cells expressed only this sustained current.

The second component of outward current was a rapidly activating transient one (inactivating within 40 msec) that began to activate at  $-38$  mV. It can be seen in Fig. 3B at potentials negative to those at which the noninactivating current turns on. The fast

transient current was strongly dependent on holding potential (*see below*); 21/65 cells expressed the fast transient outward current in addition to the sustained delayed rectifier.

The third component of outward current was a more slowly inactivating transient current that is seen predominantly at more positive potential steps (above  $+22$  mV) and was not as dependent on holding potential as the early transient current. It was expressed along with the delayed rectifier, and in the absence of the earlier transient current in 10/65 cells, as seen in Fig. 3C.

The steady-state inactivation properties of the three types of current are shown in Fig. 4. The top traces (Fig. 4A) are from a cell that expressed only the sustained delayed rectifier. Pulses to  $+32$  mV are shown, delivered from the holding potentials indicated next to the traces. Some reduction of current (steady-state inactivation) occurs between  $-88$  and  $-48$  mV, but holding potentials more positive than that did not further reduce the current past approximately 50%, as can be seen in the plot below (Fig. 4D, circles). In a different cell which expressed only the sustained current and the early transient

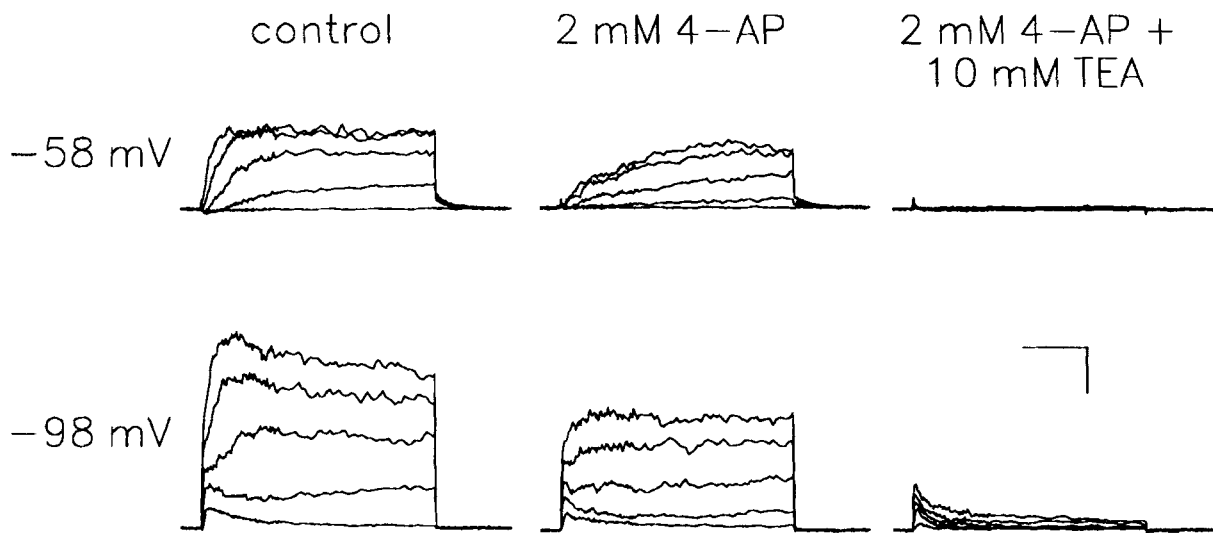


**Fig. 5.** Pharmacological separation of  $K^+$  currents. Families of currents in top row are from a holding potential of  $-58$  mV, those on the bottom row from a holding potential of  $-98$  mV. Control conditions (left column), addition of 2 mM 4-AP (middle column) and with 4-AP plus 10 mM TEA (right column). Scale bars are 50 msec and 100 pA.

current (Fig. 4B), inactivation of the fast transient current is recorded during pulses to  $-18$  mV, where the sustained current is only minimally activated. The inactivation curve (Fig. 4D, squares) is at more negative potentials than for the sustained current (the half-maximal voltage is  $-72$  mV), and has a steeper dependence on voltage (slope factor of an  $e$ -fold change in 8 mV). The slow transient current is difficult to separate from the sustained current, since they activate at similar voltages (Fig. 4C). However, its inactivation occurs at more positive potentials and is less steep than for the fast transient current (triangles, Fig. 4D).

All three components of current were present in 27/65 cells. Figure 5 shows pharmacological separation of the currents in one such cell. The lower traces are recorded from a holding potential of  $-98$  mV, and the upper traces are from  $-58$  mV. Traces during test pulses to  $-28$ ,  $-8$ ,  $+12$ ,  $+32$  and  $+52$  mV are shown. Under control conditions, a sustained component of current is recorded from a holding potential of  $-58$  mV. From a holding potential of  $-98$  mV, the two transient components of current are also seen: the slow transient component at more positive potentials is blocked by 2 mM 4-AP (compare left and middle traces); the fast early component of transient current at negative potentials is less blocked by 4-AP or TEA (compare left and right traces). The sustained component of current is blocked by 10 mM TEA. Experiments with two additional cells demonstrated block of the sustained current from a holding potential of  $-98$  mV to 57% and 21% by 5 and 15 mM TEA, respectively, while

the slow transient current was not blocked (98% and 96% remaining, respectively). These currents are all  $K^+$  selective, since the reversal potential shifted 50 mV for a tenfold change in external  $K^+$  concentration from 2.5 to 25 mM.

#### INWARD RECTIFIER

With the same recording conditions as for outward  $K^+$  currents, an inward rectifier  $K^+$  current could be activated by steps to negative potentials from holding potentials of  $-98$  or  $-78$  mV. This current was small, averaging  $-28 \pm 22$  pA/cell ( $n = 41$ ;  $-3.9 \pm 3.1$  pA/pF) at the end of a 400-msec pulse to  $-148$  mV. The current began to activate at about  $-100$  mV, and could be seen at potentials as negative as  $-190$  mV. The current was selective for  $K^+$ , as shown in Fig. 6A, where current-voltage relations recorded from one cell are shown in 2.5, 10 and 25 mM external  $K^+$ . The zero-current potential ( $E_{rev}$ ) shifts to more positive voltages with increasing external  $K^+$  concentration. The reversal potentials from five different cells are plotted in Fig. 6B, with a dashed line which corresponds to 58 mV for each tenfold change in  $K^+$  concentration. Block of the  $K^+$  inward rectifier by external  $Ba^{2+}$  ions is shown in Fig. 6C. Thus, this inward rectifier resembles that seen in other cells in that it is  $K^+$  selective, has similar voltage dependence and is blocked by low concentrations of external  $Ba^{2+}$ . In addition, this current was insensitive to the concentrations of TEA and 4-AP which were used to block outward potassium currents.

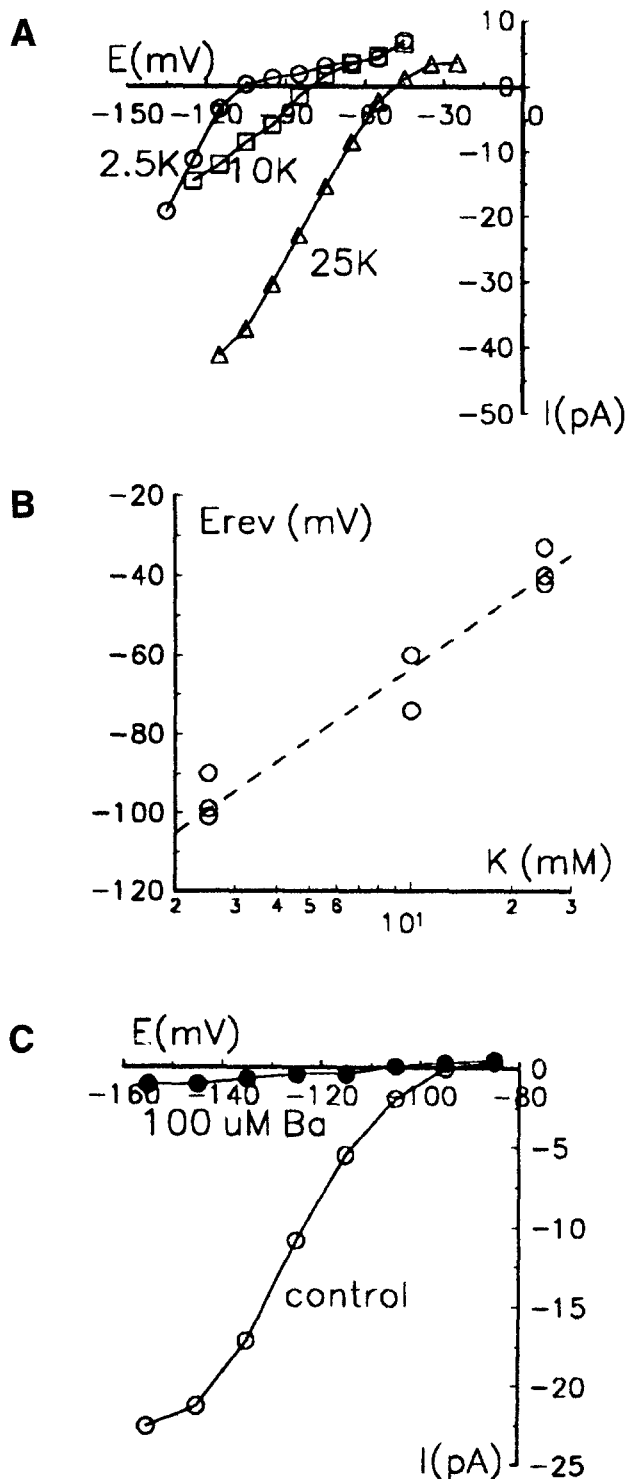


**Fig. 6.** Selectivity and blocking of inward rectifier. (A) Current-voltage relations for steady currents at the end of 400 msec steps plotted against voltage in 2.5 (circles), 10 (squares) and 25 (triangles) mM external  $K^+$ . (B) Reversal potentials for the currents from five different cells plotted semilogarithmically against the external  $K^+$  concentration (circles). Line is drawn to show Nernstian shift of 58 mV/tenfold concentration change. (C) Current-voltage relation for inward rectifier current plotted without (open circles) and with (filled circles) 100  $\mu$ M external  $Ba^{2+}$ .

The inward rectifier was also tested for modulation by several hormones. Two peptide hormones were found to modulate the current, although not in every cell. GnRH applied between 200 nM and 2  $\mu$ M suppressed the current in 10/19 cells tested, and somatostatin at similar concentrations suppressed in 8/19 cells tested. The suppression by GnRH is shown in Fig. 7. Figure 7A shows current traces in control (top) and with 1  $\mu$ M GnRH (bottom). The current elicited by steps to -108 to -168 mV is reduced by the addition of GnRH. Figure 7B shows the current-voltage relation for the suppression of the inward rectifier current in a different cell. At more positive potentials, where the currents are smaller, the current scale has been expanded tenfold for clarity (filled symbols).

#### OTHER RESPONSES

Although GABA did not modulate any of the voltage-gated channels, it did activate an outwardly rectifying conductance. This increase in conductance was seen in each of 12 cells tested with GABA ranging from 2–40  $\mu$ M. In two cells tested with two GABA concentrations, the conductance increased with the higher concentration. In two cells where the estimated equilibrium potential for chloride was -67 mV, the current reversed at -65 mV. In two cells with symmetrical Cl, the current reversed near 0 mV. These effects are consistent with GABA action through  $GABA_A$  receptors.

#### SPONTANEOUS ACTIVITY

The GT1 cell lines have been shown to release GnRH in a spontaneous and cyclical manner in culture, similar to that seen in vivo [20, 30]. Therefore, the activity of these cells under long-term current-clamp and voltage-clamp recording was investigated to determine whether an electrical basis to the spontaneous cyclical secretion could be observed. Since isolated cells plated at low density were chosen for patch-clamp recording, the endogenous currents are those of individual cells, not of a network. The nystatin perforated-patch clamp technique (see Materials and Methods) was used in voltage and current clamp, ensuring that disturbance of cytoplasmic contents would be minimized, and long-term recordings were made from single cells during very slow perfusion (0.1 ml/min) of the recording dish. All experiments were done using normal mammalian Ringer outside the cells and a K-aspartate pipette solution to most closely approximate the ionic conditions seen in normal culture conditions. The time scale of all recordings was referred to the moment

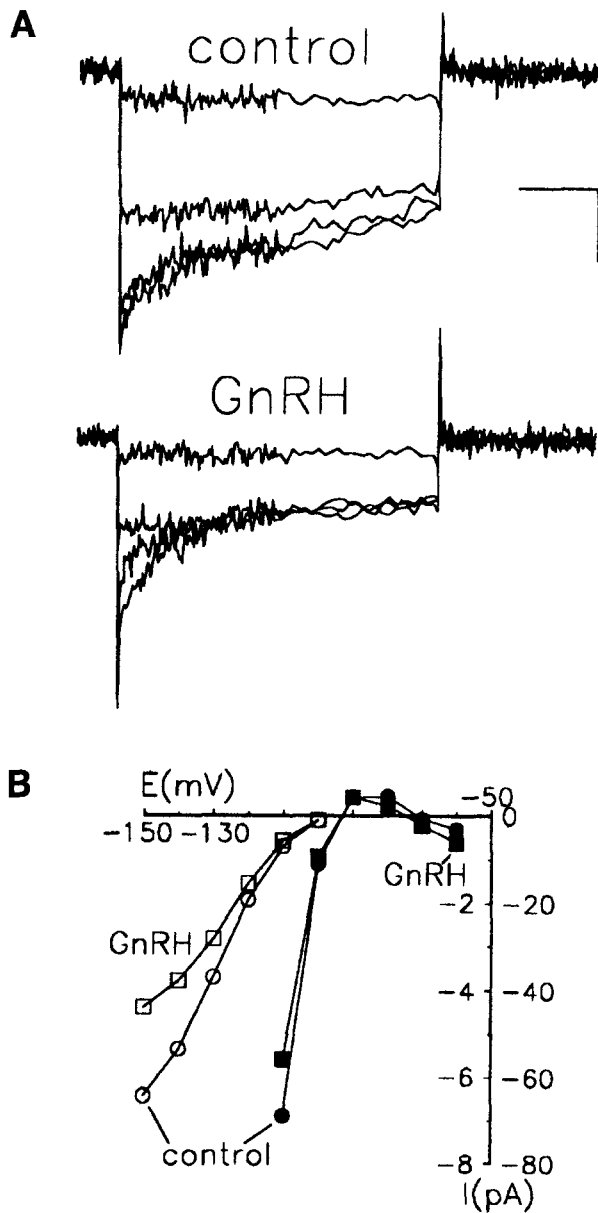


**Fig. 7.** Suppression of inward rectifier by GnRH. (A) Current traces from holding potential of  $-98$  mV to steps from  $-108$  to  $-168$  mV during control conditions (top traces) and with  $1 \mu\text{M}$  GnRH (bottom traces). (B) In a different cell, current-voltage relation is shown for control (circles) and  $200 \text{ nM}$  GnRH (squares). For potentials more positive than  $-140$  mV, data points are replotted on an expanded current scale (left side of vertical axis) and symbols are filled.

when the cells were transferred from serum- and steroid-containing culture medium to normal Ringer (time = 0).

Figure 8A shows records taken in current clamp during long-term recordings from two different cells. Because the cells had varying resting potentials after

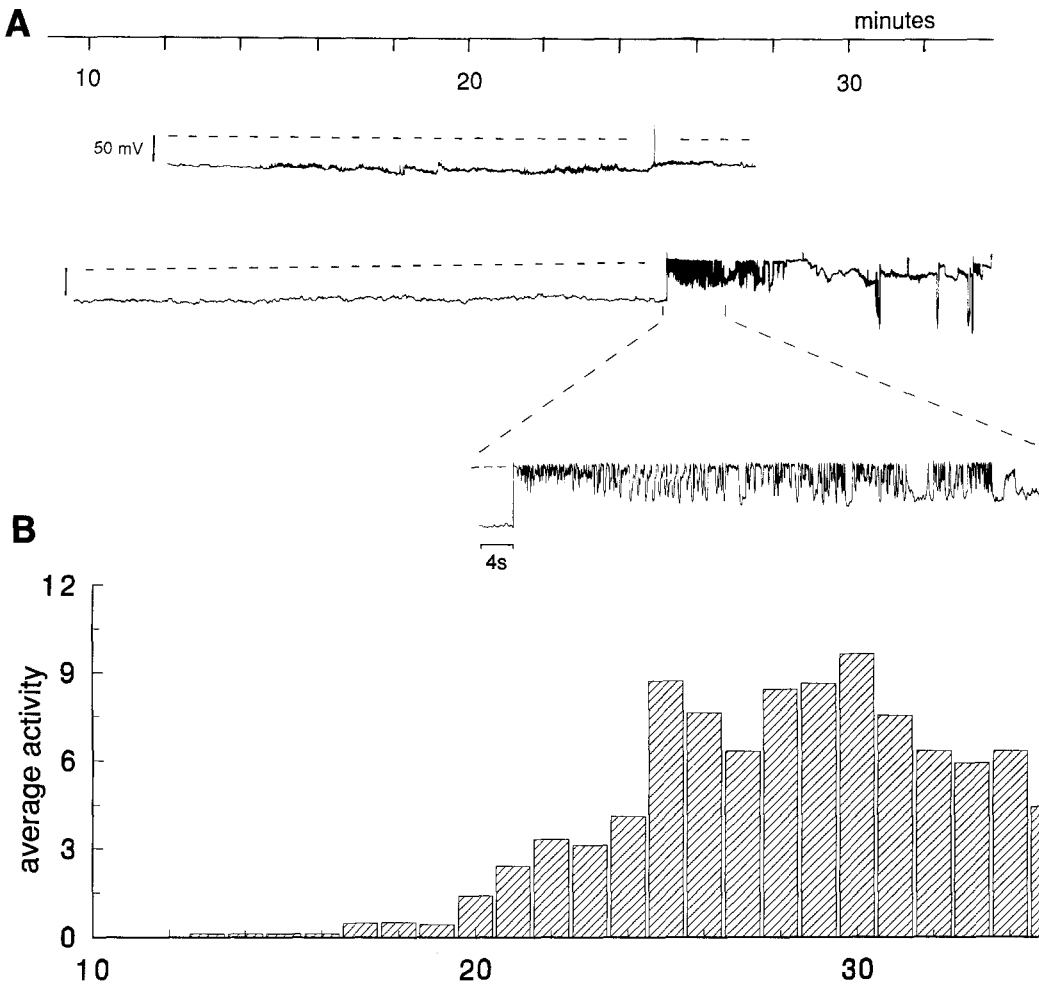
establishing the perforated patch clamp (ranging from  $-45$  to  $-70$  mV), a small amount of current was injected to polarize all the cells to near  $-70$  mV during the recording, which was the same potential used for voltage-clamp experiments under the same conditions (see below). If the amount of injected current had to be changed more than  $7$  pA or exceeded  $20$  pA, the experiment was discarded. The voltage traces from each of the cells shown was started upon successful establishment of the recording. The first cell was mostly silent, firing no action potentials, with some baseline noise, until approximately  $25$  min, when it fired one action potential and depolarized slightly. The recording was then lost. The second cell was completely quiet until  $25$  min, when it fired a long oscillatory burst, part of which is shown on a faster time scale below.

Figure 8B is a histogram of mean activity recorded under nystatin current-clamp conditions for the 26 cells from which successful recordings were made (by above criteria) between  $10$  and  $35$  min after removing the cells from culture medium (see figure legend for details on quantification of depolarizing activity). The histogram shows that the average activity increased during the interval of  $20$ – $35$  min.

A similar series of experiments was performed under nystatin perforated-patch voltage clamp to determine the ionic basis of this increase in activity. During these experiments, the membrane potential was clamped to  $-70$  mV, and a rapid series of pulses ranging from  $-80$  to  $+11$  mV was given every  $30$  sec to determine the reversal potential of any ionic events which occurred. The brief current deflections associated with these pulses have been removed from the current traces to minimize confusion. Figure 8C shows long-term current records from two cells. The first cell is quiet until  $20$  min, when an inward spike of current is seen. A similar event occurred at  $29$  min in the second cell shown. The inward current oscillations are expanded on a faster time scale for clarity. Of  $15$  cells recorded under voltage clamp,  $13$  cells had inward current activity during the interval of  $19$ – $32$  min after being taken out of serum-containing medium.

The currents resulting from the rapid voltage steps given during the voltage-clamp recordings were analyzed by averaging those recorded during periods of activity and subtracting from those averaged records recorded during silent periods. These were then plotted against voltage, giving a current-voltage relation for the endogenous current arising during spontaneous ionic activity. Fits of six cells gave a mean reversal of  $-15 \pm 9$  mV of this activity. This suggests that the ionic basis of this activity is not  $\text{Ca}^{2+}$  or  $\text{Na}^+$  (reversal potentials above  $+40$  mV) or  $\text{K}^+$  (reversal potential below  $-80$  mV). The rever-





**Fig. 8.** Spontaneous voltage activity in nystatin-clamped cells. Time scales indicate minutes, with time = 0 being the point at which the cells were removed from serum- and steroid-containing tissue culture medium, rinsed for 30 sec with zero-divalent Ringer, and perfused with normal mammalian Ringer. (A) Current clamp. Scale bar indicates 50 mV, and the dashed line indicates  $-10$  mV. Expanded portion of traces for second cell is shown by dotted lines. (B) Average depolarizing activity plot for 26 cells in current-clamp mode. The depolarizing activity was calculated by measuring the number of action potentials or calculating depolarizing units as follows: The mean area under an action potential was  $120$  mV-sec. A depolarization of  $20$  mV for  $6$  sec was taken to be the same total depolarization ( $20$  mV) $\times$ ( $6$  sec) and set to equal 1 action potential. The total activity was averaged over 3-min bins. The standard deviations of the means are not plotted since the dynamic range of the data is so high (e.g., some cells increased from  $0$ – $0.6$  spikes/min while others changed from  $0$ – $35$  spikes/min). (C) Voltage clamp. Scale bars here indicate  $5$  pA, and cells were held at  $-70$  mV for the duration of the recordings. Expanded portions of traces are shown by dotted lines.

sal potential for  $\text{Cl}^-$  is unknown under these conditions, since it is sparingly permeable in nystatin pores. Thus, the current activated may be due to a nonspecific cation conductance or perhaps to a  $\text{Cl}$  conductance.

In some cells in which the recordings lasted for more than one hour, spontaneous activity seemed to be repeated. One cell showed an episode of activity from approximately 23–30 min, followed by relative silence and another episode of activity from 48–60 min. The activity seemed to be diminishing again when the recording was lost. This may indicate a cycle of activity with a 26-min interval. In another

cell, action potentials were recorded in current clamp at 20 min, and again at 40–43 min. The recording was then switched to voltage-clamp mode, and at approximately 63 min inward currents were seen which then diminished. The recording continued to past 70 min. This could represent a cycle of activity with approximately 21-min intervals.

### Discussion

Several laboratories have shown that the GT1 cell lines generated in transgenic mice are useful for stud-

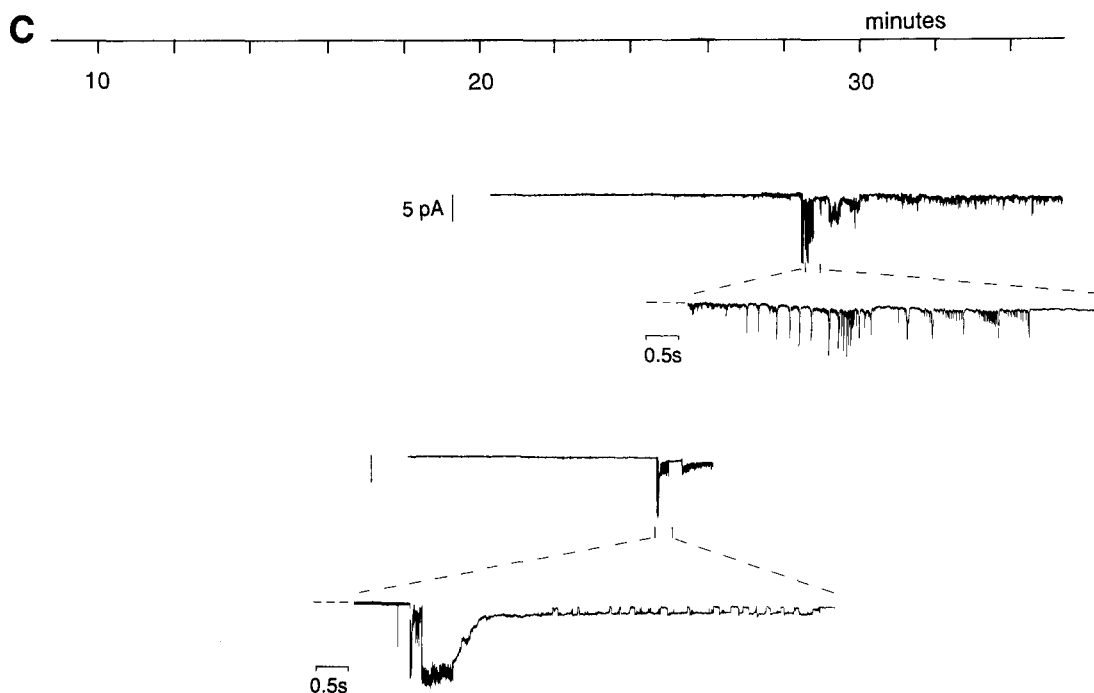


Fig. 8. Continued.

ies of GnRH secretion and regulation. In part they compensate for the unavailability of homogeneous primary GnRH neuron cultures. The GT1 cells secrete GnRH in a pulsatile manner in perfused culture systems [20, 30]; there are cell-cell junctional contacts and synapses as seen in vivo [29, 30]; and secretion of GnRH is dependent on external  $\text{Ca}^{2+}$  as has been shown in experiments on slices from rat hypothalamus [6, 20, 30]. In addition, secretion of GnRH from GT1 neurons is modulated by activin-A [8], which has been shown to play a role in secretion of FSH [18], and by endothelin (via  $\text{IP}_3$  and  $\text{Ca}^{2+}$ -mobilization) in a manner similar to that seen in hypothalamic neurons [15]. These experiments demonstrated that periodic GnRH secretion does not require the complex interactions with other neuronal subtypes found in the brain, but is a property intrinsic to the network of GnRH cells themselves [20, 30].

In castrated rats, GnRH is secreted approximately every 30 min from the median eminence into the portal circulation [21], eliciting synchronous LH secretion [7]. Periodic secretion from perfused GT1 cell cultures at  $37^\circ\text{C}$  has an interpeak interval of 26 min [20] or 36 min [30]; this difference in the interval may depend on the perfusion medium or on the specific GT1 cell line used. The electrophysiological experiments presented here suggest an intrinsic periodicity of 20–30 min at  $23^\circ\text{C}$ . Although the temperature is lower, the interval is similar to that seen in perfusion experiments. Little is known about the

temperature dependence of secretion of GnRH. It is possible that the differences in culture conditions have an effect on the GnRH secretion. In addition, the perfusion work was done with cultures that were far more confluent than those used in the present work (50–70% vs. 10–15% confluent).

The present experiments demonstrate that GT1 neurons in saline solutions can maintain a resting membrane potential between  $-70$  and  $-45$  mV and produce relatively long action potentials. The  $\text{Na}^+$  current expressed in these cells inactivates at potentials similar to those recorded from primary septal neurons [4]. Thus, a relatively large proportion of the  $\text{Na}^+$  current is available for action potential production from a depolarized resting potential. It is probable that  $\text{Na}^+$  is the major ion species involved in the upstroke of the action potential, since the transient type of Ca channel, which could participate in a similar way [9], is expressed at relatively low density in GT1 cells. In addition, GnRH secretion from these cells and from hypothalamic explants in culture has been shown to be TTX sensitive [6, 22]. The influx of calcium is, therefore, through the sustained Ca channels. Secretion of GnRH from the cell lines and from primary hypothalamic explants is dependent on external  $\text{Ca}^{2+}$ , and is blocked by removal of external  $\text{Ca}^{2+}$  [6, 20, 30] and by an organic Ca channel blocker which implicates L-type Ca channels in the secretion [6].

Repolarization of the action potential is carried out via activation of the sustained delayed rectifier

$K^+$  current, which activates with a time course of 15–20 msec at the more positive potentials. This is relatively slow compared to many other delayed rectifiers (2–3 msec; [10]) thus permitting a long action potential in these neurosecretory cells.

The experiments presented here suggest two different mechanisms that could be involved in synchronous secretion of GnRH both by the GT1 cells in culture, and perhaps also in vivo in a network of neurons that may have processes in contact with each other. One possible mechanism is that secretion of GnRH by one cell reduces the inward rectifier current in other GnRH neurons in proximity to the secreting cell, rendering them more excitable. Such positive feedback is seen, for example, in rat nucleus basalis neurons, where substance P suppresses a similar inward rectifier, leading to a long-lasting increase in excitability [33]. In addition, the cells may have an endogenous oscillator, which turns on an inward excitatory conductance. Since this is seen during slow perfusion with low cell density in the experiments presented here, it is not likely to require an extracellular messenger. This “endogenous oscillator” would tend to cause each cell to fire periodically. Coordination of GnRH secretion from intrinsically periodic cells in vivo could depend both on the positive feedback from GnRH and on electrical coupling at cell-to-cell junctions. Both mechanisms may be particularly active at the median eminence where processes of many GnRH neurons converge.

The suppressing effect of GnRH on the inward rectifier would suggest a positive feedback on GnRH secretion. This is in contrast to reports in which administration of GnRH to the preoptic area in vivo or to explanted hypothalami have demonstrated an “ultrashort” feedback loop of GnRH decreasing GnRH and LH secretion [27, 34]. It is possible that the responses to sustained administration of GnRH are different from that seen with endogenous pulsatile GnRH or that the concentrations of GnRH are different in the two cases.

In addition to these mechanisms, the importance of the modulation of other networks that impinge on the GnRH neuron system cannot be overlooked. Neurons containing glutamic acid decarboxylase, an enzyme present in GABAergic cells, have been demonstrated to form symmetrical synapses with GnRH-containing neurons [16]. Measurements of GABA from the preoptic area in rats have shown that the levels of GABA decrease immediately preceding an LH surge [13], and GABA injected into the preoptic area decreased secreted LH and abolished the pulsatile release of LH [12]. The same studies suggested that an oscillation in GABA concentration in the preoptic area synchronizes the activity of GnRH neurons to generate GnRH pulses. Since the GT1 cultures are clonal and do not contain the GABA

neurons, this mechanism for GnRH periodic secretion is not operable. However, the cells do express a  $GABA_A$  response which, in vivo, would allow GABAergic inputs to modulate secretion. Thus, although GnRH neurons cells possess an intrinsic or endogenous oscillator, the final periodicity of GnRH secretion must also be shaped by cell-cell interactions between GnRH neurons, and by modulation of output by additional networks which interact with the GnRH neuron network.

This work was supported by a Research Award from the McKnight Foundation and NIH grant NS08174 to B. Hille, and by a training grant NS07097 and NRSA NS08868 to MMB. I would like to thank Dr. G. Stanley McKnight for use of tissue culture facilities, Drs. Michael Barish, Pamela Mellon, Robert Steiner and William Moody for helpful discussions, and Bertil Hille and William Moody for reading the manuscript. I would also like to thank Dr. Bertil Hille for encouragement and laboratory space to perform the work reported here.

## References

1. Bean, B.P. 1989. Classes of calcium channels in vertebrate cells. *Annu. Rev. Physiol.* **51**:367–384
2. Bezanilla, F., Armstrong, C.M. 1977. Inactivation of the sodium channel: I. Sodium current experiments. *J. Gen. Physiol.* **70**:357–365
3. Carmel, P.W., Araki, S., Ferin, M. 1976. Pituitary stalk portal blood collection in Rhesus monkeys: evidence for pulsatile release of gonadotropin releasing hormone (GnRH). *Endocrinology* **99**:243–248
4. Castellano, A., Lopez-Barneo, J. 1991. Sodium and calcium currents in dispersed mammalian septal neurons. *J. Gen. Physiol.* **97**:303–320
5. Clarke, I.J., Cummins, J.T. 1982. The temporal relationship between gonadotropin releasing hormone (GnRH) and luteinizing hormone (LH) secretion in ovariectomized ewes. *Endocrinology* **111**:1737–1739
6. Drouva, S.V., Epelbaum, J., Hery, M., Tapia-Arancibia, L., Laplante, E., Kordon, C. 1981. Ionic channels involved in the LHRH and SRIF release from rat mediobasal hypothalamus. *Neuroendocrinology* **32**:155–162
7. Gay, V.L., Sheth, N.A. 1972. Evidence for a periodic release of LH in castrated male and female rats. *Endocrinology* **90**:158–162
8. Gonzalez-Manchon, C., Bilezikjian, L.M., Corrigan, A.Z., Mellon, P.L., Vale, W. 1991. Activin-A modulates gonadotropin-releasing hormone secretion from a gonadotropin-releasing hormone-secreting neuronal cell line. *Neuroendocrinology* **54**:373–377
9. Hagiwara, N., Irisawa, H., Kameyama, M. 1988. Contribution of two types of calcium channels to the pacemaker potentials of rabbit sino-atrial node cells. *J. Physiol.* **359**:233–253
10. Hille, B. 1992. *Ionic Channels of Excitable Membranes*. Sinauer Associates, Sunderland, MA
11. Horn, R., Marty, A. 1988. Muscarinic activation of ionic currents measured by a new whole-cell recording method. *J. Gen. Physiol.* **92**:145–159
12. Jarry, H., Leonhardt, S., Wuttke, W. 1991. Gamma-aminobutyric acid neurons in the preoptic/anterior hypothalamic

- area synchronize the phasic activity of gonadotropin-releasing hormone pulse generator in ovariectomized rats. *Neuroendocrinology* **53**:261-267
13. Jarry, H., Perschl, A., Wuttke, W. 1988. Further evidence that preoptic anterior hypothalamic neurons are part of the GnRH pulse and surge generator. *Acta Endocrinol.* **123**: 573-579
  14. Kalra, S.P., Kalra, P.S. 1983. Neural regulation of luteinizing hormone secretion in the rat. *Endocrine Rev.* **44**:331-351
  15. Krsmanovic, L.Z., Stojilkovic, S.S., Balla, T., Al-Damluji, S., Weiner, R.I., Catt K.J. 1991. Receptors and neurosecretory actions of endothelin in hypothalamic neurons. *Proc. Natl. Acad. Sci. USA* **88**:11124-11128
  16. Leranthe, C., MacLusky, N.J., Sakamoto, H., Shanabrough, M., Naftolin, F. 1985. Glutamic acid decarboxylase-containing axons synapse on LHRH neurons in rat medial preoptic area. *Neuroendocrinology* **40**:536-539
  17. Levine, J.E., Ramirez, V.D. 1982. Luteinizing hormone-releasing hormone release during the rat estrous cycle and after ovariectomy, as estimated with push-pull cannulae. *Endocrinology* **111**:1439-1448
  18. Ling, N., Ying, S.H., Ueno, N., Shimasaki, S., Esch, F., Hotta, M., Guillemin, R. 1986. Pituitary FSH is released by a heterodimer of the  $\beta$ -subunits from the two forms of inhibin. *Nature* **321**:779-782
  19. Liposits, I., Merchenthaler, I., Wetsel, W.C., Reid, J.J., Mellon, P.L., Weiner, R.I., Negro-Vilar A. 1991. Morphological characterization of immortalized hypothalamic neurons synthesizing luteinizing hormone-releasing hormone. *Endocrinology* **129**:1575-1583
  20. Martinez de la Escalera, G., Choi, A.L., Weiner, R.I. 1992. Generation and synchronization of gonadotropin-releasing hormone (GnRH) pulses: intrinsic properties of the GT1-1 GnRH neuronal cell line. *Proc. Natl. Acad. Sci. USA* **89**:1852-1855
  21. Masotto, C., Negro-Vilar, A. 1988. Gonadectomy influences the inhibitory effect of endogenous opiate system on pulsatile gonadotropin secretion. *Endocrinology* **123**:747-752
  22. Mellon, P.L., Windle, J.J., Goldsmith, P.C., Padula, C.A., Roberts, J.L., Weiner, R.I. 1990. Immortalization of hypothalamic GnRH neurons by genetically targeted tumorigenesis. *Neuron* **5**:1-10
  23. Negro-Vilar, A., Valenca, M.M., Culler, M.D. 1987. Transmembrane signals and intracellular messengers mediating LHRH and LH secretion. *Adv. Exp. Med. Biol.* **219**:85-108
  24. Plant, T.M. 1986. Gonadal regulation of hypothalamic gonadotropin-releasing hormone release in primates. *Endocrine Rev.* **7**:75-88
  25. Pohl, C.R., Knobil, E. 1982. The role of the central nervous system in the control of ovarian function in higher primates. *Annu. Rev. Physiol.* **44**:583-593
  26. Silverman, A.-J. 1988. The gonadotropin-releasing hormone (GnRH) neuronal systems: Immunocytochemistry. In: *The Physiology of Reproduction*. E. Knobil, and J.D. Neill, editors. Raven, New York
  27. Valenca, M.M., Johnston, C.A., Ching, M., Negro-Vilar, A. 1987. Evidence for a negative ultrashort feedback mechanism operating on the luteinizing hormone-releasing hormone neuronal system. *Endocrinology* **121**:2256-2259
  28. Weiner, R.I., Findell, P.R., Kordon, C. 1988. Role of classic and peptide neuromediators in the neuroendocrine regulation of LH and prolactin. In: *The Physiology of Reproduction*. E. Knobil, and J.D. Neill, editors. Raven, New York
  29. Wetsel, W.C., Mellon, P.L., Weiner, R.I., Negro-Vilar, A. 1991. Metabolism of pro-luteinizing hormone-releasing hormone in immortalized hypothalamic neurons. *Endocrinology* **129**:1584-1595
  30. Wetsel, W.C., Valenca, M.M., Merchenthaler, I., Liposits, Z., Lopez, F.J., Weiner, R.I., Mellon, P.L., Negro-Vilar, A. 1992. Intrinsic pulsatile secretory activity of immortalized luteinizing hormone-releasing hormone-secreting neurons. *Proc. Natl. Acad. Sci. USA* **89**:4149-4153
  31. Wilson, R.C., Kesner, J.S., Kaufman, J.-M., Uemura, T., Akema, T., Knobil, E. 1984. Central electrophysiological correlates of pulsatile luteinizing hormone secretion in the Rhesus monkey. *Neuroendocrinology* **39**:256-260
  32. Witkin, J.W., Paden, C.M., Silverman, A.-J. 1982. The luteinizing hormone-releasing hormone (LHRH) systems in the rat brain. *Neuroendocrinology* **35**:429-438
  33. Yamaguchi, K., Nakajima, Y., Nakajima, S., Stanfield, P. 1990. Modulation of inwardly rectifying channels by substance P in cholinergic neurones from rat brain in culture. *J. Physiol.* **426**:499-520
  34. Zanis, M., Messi, E., Motta, M., Martini, L. 1987. Ultrashort feedback control of luteinizing hormone-releasing hormone secretion *in vitro*. *Endocrinology* **121**:2199-2204